Performance Evaluation of a VLC System when Considering the Receiver's Orientations

Tayebe Ganjian,
Department of Electrical Engineering,
University of Guilan,
Rasht, Iran, 4199613776
tganjian@msc.guilan.ac.ir

Gholamreza Baghersalimi,
Department of Electrical Engineering,
University of Guilan,
Rasht, Iran, 4199613776
bsalimi@guilan.ac.ir

Zabih Ghassemlooy,
Optical Communications Research Group, Faculty of Engineering and Environment, Northumbria University
Newcastle upon Tyne, UK, NE1 8ST
z.ghassemlooy@northumbria.ac.uk

Abstract—**Visible light communications is a promising technology, which utilizes visible light for illumination, data communications, and indoor localization. For data communications and indoor positioning applications in an indoor environment, the link performance is influenced by the orientation of the receiver's plane. In this paper, we consider single-input single-output (SISO) and multiple-input single-output (MISO) systems and evaluate their performances in terms of the received optical power level by considering the receiver's orientation. For the MISO system, two different transmitter arrangements are investigated and compared. The results show that MISO offers improved performance and rotation flexibility when compared to SISO.**

Keywords- visible light communication, receiver orientation, received power

I. INTRODUCTION

In recent years, there has been a rapid increase in wireless data traffic and this exponential increase is predicted to cause serious problems with the existing radio frequency (RF) spectrum. Visible light communications (VLC) is an alternative complementary technology to the RF in addressing the spectrum shortage in certain applications. VLC is a wireless technology, which uses the visible band of the electromagnetic spectrum for data communications. With the developments in solid state lighting technology, light emitting diodes (LEDs) have become very popular and in recent years, are predicted to become the dominant light source in the future at a global level. LEDs have a unique fast switching feature compared to the other standard lights, thus enabling high-speed data transmission. In contrast to the RF technologies, where additional transceiver modules are needed in order to establish wireless connectivity, the VLC technology uses the existing LED based lighting fixtures within indoor environments to provide data communications [1, 2, 3].

Indoor VLC systems generally use the LED light sources placed on the ceiling, which can be used for illumination, data communications and also indoor positioning. In most cases, it is assumed that, the receiver (Rx) plane is facing upward towards the transmitters (Txs). However, in a more realistic scenario, the users may hold their smart-phone (i.e., Rx) in any orientations with respect to the Tx plane. The orientation of the Rx will affect the captured light intensities (i.e., received optical power level P_r). There have been several works investigating the Rx orientations. In [4] the impacts of a VLC Rx, which was worn by a moving person, was investigated by considering two different situations (*i*) the Rx's orientation was fixed; and (*ii*) a mobile Rx (i.e., different orientations). The results illustrated that, changing the orientations led to decrease in the minimal transmit power required to achieve a given outage probability at high data rates. In [5] an algorithm was investigated for mobile phone localization based on indoor VLC, where the phone's position was determined by using the estimated angle deviation. In [6] a Camera-based VLC (CVLC) system was studied considering different rotation angles (i.e., 90°, 180°, and 270°). In order to compensate for the Rx's orientations, and time synchronization, special header frames were utilized, which contained rotation and alignment markers. In [7] an infrastructure-to-car communications based on VLC was investigated, where the Tx was fixed while the detector was rotated in order to improve the reception region. The Tx tracked the RX with the Rx selecting path with the largest power level. In [8] a method was proposed for estimating the Rx's rotation angles in an indoor VLC navigation system. Authors in [9] investigated a new approach for access point selection, where one of the considered parameters was the mobile station orientation. In [10] authors proposed a visible light positioning (VLP) system utilizing a single LED for transmission and a smartphone camera as the Rx. The Rx's position and orientation was determined and used for compensating the angular sensor dependence of the image sensor. In [2] channel modeling in VLC systems was studied in Chapter 6, and VLC systems were investigated for different indoor environments by determining the channel impulse response and the delay time. Authors considered different scenarios including empty and furnished rooms, different Tx and Rx arrangements, and also Rx rotation. In [11] a VLC system was investigated considering random mobility and rotation of an Rx to determine the probability of handover and also handover rate. In [12] two MISO models for the Tx's configuration, i.e., the corner and axis excited topologies, were investigated. Results showed that the axis excited topology offered improved performance in terms of root mean square (RMS) delay profiles. In [13] P_r profile for the SISO VLC system based on the Tx's position was studied.

So far, there have been several researches carried out on the Rx's orientation in VLC systems, but to the best of our knowledge no investigation on different Tx's configurations has been reported. In this paper, we further investigate P_r for the SISO and MISO based VLC system by considering the Rx's orientations, and determine the minimum detectable P_r at the Rx. For the MISO system, we investigate two different transmitter arrangements and compare their performances. We show that, MISO offers improved performance and rotation flexibility when compared to SISO. The rest of the paper is organized as follows. In Section II, the system orientation model and rotation angles are introduced where the rotation is divided into two main components. In Section III, different topologies are discussed including SISO, MISO corner excited, and MISO axis excited. The System performance is investigated in Section IV followed by conclusion in Section V.

II. System Model

Fig. 1 shows the orientation model in a SISO-VLC system where Tx is positioned on the ceiling center and the Rx is located on a table. x, y and z, respectively show the room length, width and height. Generally, in most VLC scenarios, both the Rx and the Tx planes are assumed to be parallel, which is shown by the dashed lines in Fig. 1. Here, the Rx with no rotation is aligned with the Tx with the field of view (FOV) of φ while solid lines illustrate the rotated Rx with the new FOV of φ_r.

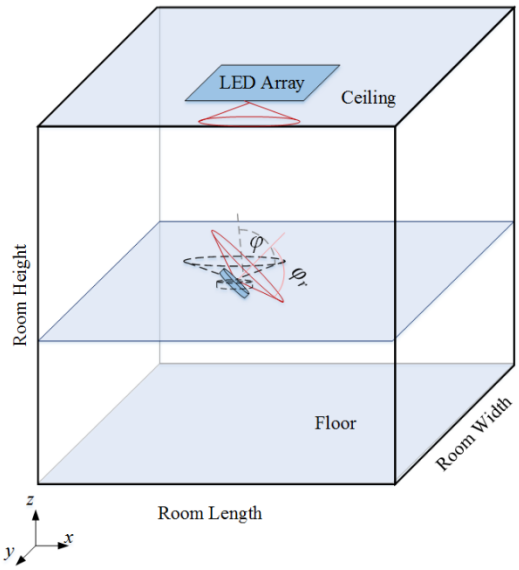

Fig. 1- VLC rotation model

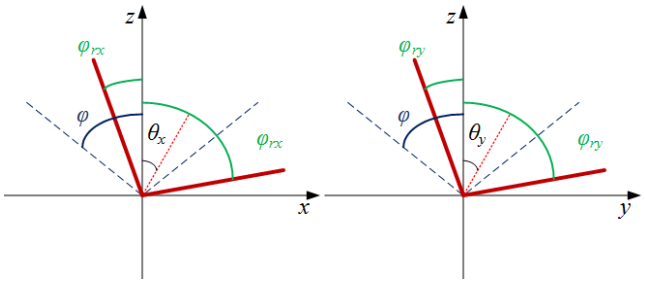

Fig. 2- The Rx rotation in the x-z and y-z planes

TABLE I. SIMULATION PARAMETERS

Parameter	Value
Room dimensions	5×5×3 m^3
Tx position (SISO)	(0 0 3) m
Tx position (corner excited)	(±1.25, ±1.25, 3) m
Tx position (axis excited)	(±1.25, 0, 3) , (0, ±1.25, 3) m
Number of LEDs	10 × 10
LED semi-angle at half power	70°
Single LED transmit power	20 mW
Rx FOV	70°
Photodetector area	0.1 cm^2
Receiver sensitivity	-30 dBm

A. Calculating the rotation angles

In order to determine the rotation impacts on the link performance, the rotation angle is decomposed into two main components of the rotation angle around the x-axis in the y-z plane and the rotation angle around the y-axis in the x-z plane. Fig. 2 shows the rotation angles in the x- z and y-z planes. θ_x is the FOV rotation in the x-z plane around the y-axis while ϕ_{rx} shows the new FOV of the Rx in the x-z plane by considering rotation effects. θ_y and ϕ_{ry} are also, respectively, the rotation angles around the z-axis in the y-z plane and the new FOV in the y-z plane, respectively.

The SISO and MISO based VLC systems are investigated for a typical room of a dimension of (5×5×4) m^3. The Tx is an LED array of 10×10. For SISO, the Tx is placed at the center of the ceiling (i.e. (0, 0, 3) m) while the Rx is located on a table 0.85 m above the floor. The key system parameters are given in
Table I. The rotated FOV φ_r depends on the positions of both the Tx and the Rx, which is given as:

$$\varphi_r = \begin{cases} \varphi + \theta_x + \theta_y, & x_R > x_T, y_R > y_T \\ \varphi + \theta_x - \theta_y, & x_R > x_T, y_R < y_T \\ \varphi - \theta_x + \theta_y, & x_R < x_T, y_R > y_T \\ \varphi - \theta_x - \theta_y, & x_R < x_T, y_R < y_T \end{cases} . \quad (1)$$

In this paper, SISO and MISO based VLC systems are investigated and P_r is calculated for different positions of the Rx in the x-y plane by considering the Rx orientation. The minimum P_r is then evaluated for each position. For SISO, the Tx is positioned at a location of (0, 0, 3) m, while for MISO two different 4×1 Tx arrangements are studied, including the corner excited and the axis excited topologies. For the corner excited scenario, the Tx arrangement, which is illustrated in Fig. 3(a), has a rectangular pattern where the Txs are located at (±1.25, ±1.25, 3) m. But, for the axis excited topology, the Txs are placed on the x and y axes at (±1.25, 0, 3) and (0, ±1.25, 3) m, respectively. The Tx arrangement of the axis excited model is shown in Fig. 3(b).

III. Results and Discussions

In order to determine the limits on the Rx's rotation angles for each Rx position, we calculate (*i*) P_r for a range of rotation

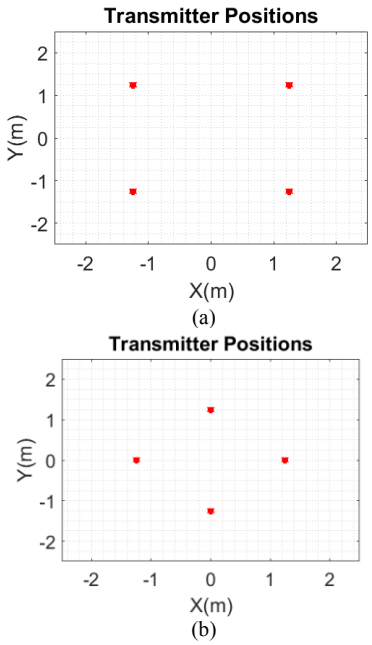

Fig. 3- MISO Tx arrangement: (a) corner excited, and (b) axis excited

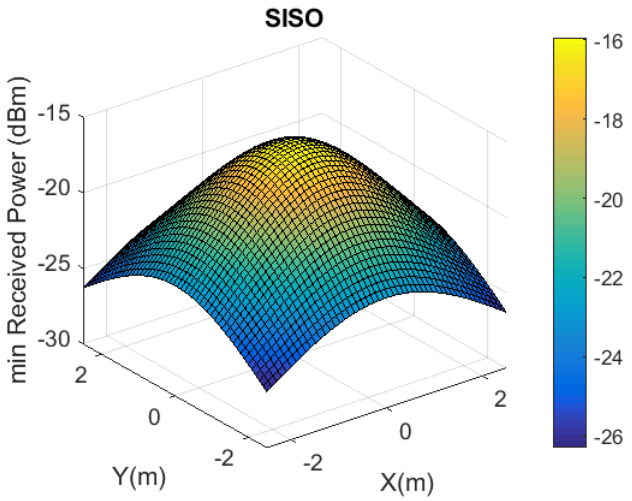

Fig. 4- The minimum P_r in the *x*-*y* plane for SISO

angles; (*ii*) the minimum P_r at the Rx; and (*iii*) the attributed rotation angle. Fig. 4 shows the minimum P_r in the *x*-*y* plane for SISO. The *x*- and *y*-axis show the room's length and width, respectively. Note that, the darker colors represent lower power levels. It is shown that the minimum P_r has a symmetric pattern with a peak value of -15.94 dBm at the Rx's position of (0, 0, 0.85) m where the Rx is completely aligned with the Tx. The limitation of the Rx's rotation angle in the *x*-axis, which leads to the minimum detectable P_r in the *x*-*z* plane for SISO is shown in Fig. 5 (a). Note that, in areas near the center e.g., (-0.5, 0, 0.85) m, the rotation limit is -65° and if the rotation angle values are lower than the predicted values, then P_r will be lower than the receiver sensitivity (i.e., by -30 dBm) and therefore there will be no data transmission. Fig. 5 (b) shows the *y*-rotation angle limits in the *y*-*z* plane for SISO. It is observed that the minimum P_r for

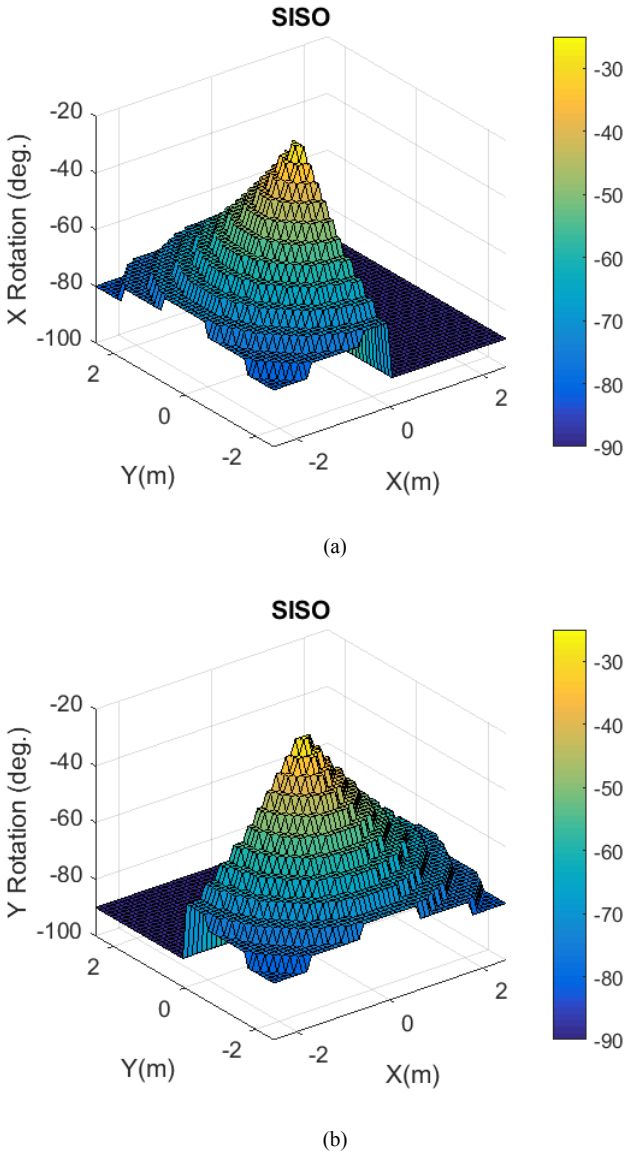

Fig. 5- The rotation angle limit for SISO for (a) *x*-axis, and (b) *y*-axis

the areas with positive position on the *x* axis is achieved in -90° rotation degree. It is also observed that due to the symmetric Tx arrangement, Fig. 5(b), which illustrates rotation angle limits in the *y*-*z* plane, has a similar pattern to the angle limits in the *x*-*z* plane (see Fig. 5(a)) with 90° rotation in the *x*-*y* plane. It is obvious that for every positions, the Rx should be oriented towards the Tx, which is located at (0, 0, 3) m, in order to receive a detectable P_r. Therefore, in areas with positive *x* and *y*, it is reasonable to have negative rotation angles. It is also observed that, in these areas, among the detectable values of P_r the minimum value is related to the rotation angle of -90° where both the Rx and the Tx planes are vertical. Fig. 6 shows the minimum P_r for MISO for the corner excited Tx pattern. The

transmit power of each Tx is divided by 4, which represent the power per SISO. Compared to SISO, as shown in Fig. 4, it is observed that, P_r in the center of the room is considerably decreased from -15.6 to -23 dBm. It is also observed that, the maximum value of P_r for the corner excited pattern is -20 dBm,

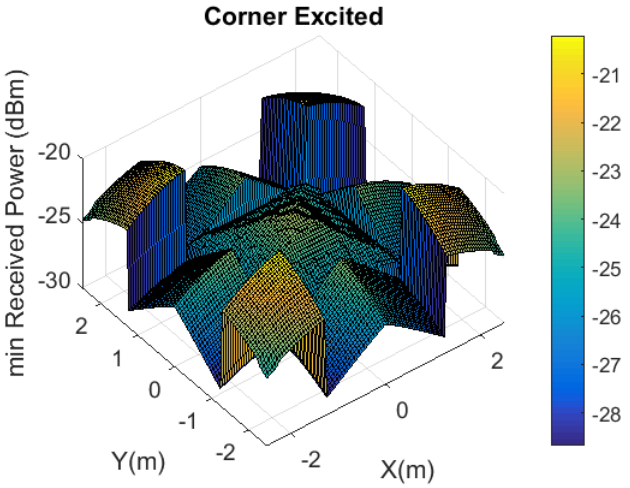

Fig. 6- The minimum P_r at the corner of the room excited Tx pattern

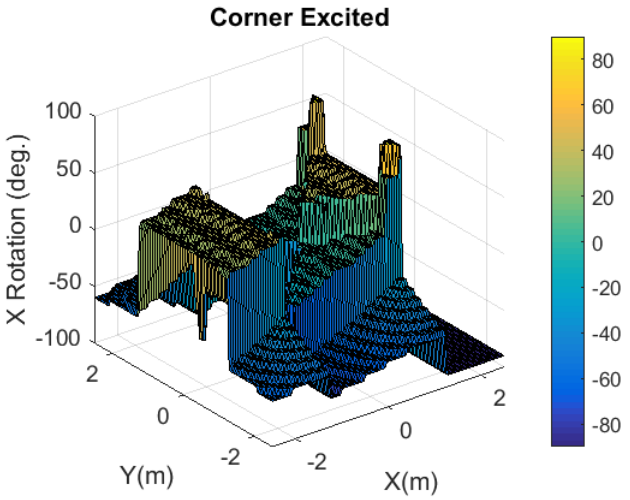

Fig. 7- Rotation angle limit in x-z plane for corner excited Tx pattern

which is lower by 4 dBm compared to SISO. For MISO with the Txs located in the corner of the room, the highest P_r is observed at the location of (±1.25, ±1.25, 0.85) m, which are the closest positions to the Txs. But, each Tx has a power four times lower than the SISO Tx, and this is the reason why the maximum P_r in this topology is lower compared to SISO. It is also observed in Fig. 6 that, the minimum detectable P_r is increased in the corners because the Txs are closer to corners in this scenario compared to SISO.

Fig. 7 depicts the rotation angles in the x-z plane, which shows the minimum detectable P_r in each position for the corner excited Tx pattern. Note that, in this topology the Tx is not at the center of the ceiling. Therefore, it is observed that, for the Rx's position at the center of the x-y plane i.e., (0, 0, 0.85) m, rotating the Rx toward any Tx increases P_r. As a result, the minimum P_r is observed for the zero rotation angle for this position. For the Rx's position of (-0.5, 0, 0.85) m the minimum P_r is achieved for the rotation angle of -50° in the x-z plane, while for (-2, -2, 0.85) m the angle is -55°. This is because of the symmetry, where

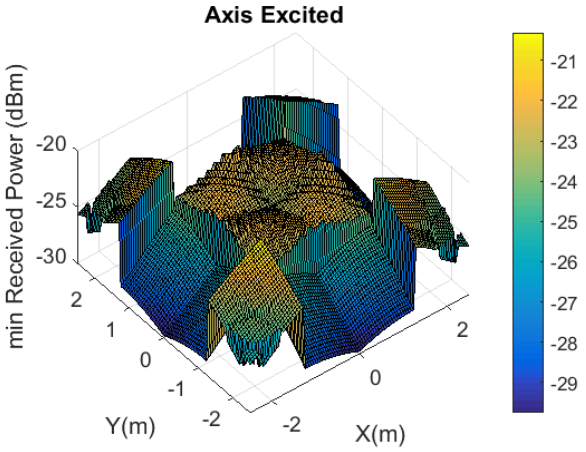

Fig. 8- The minimum P_r in the axis excited Tx pattern

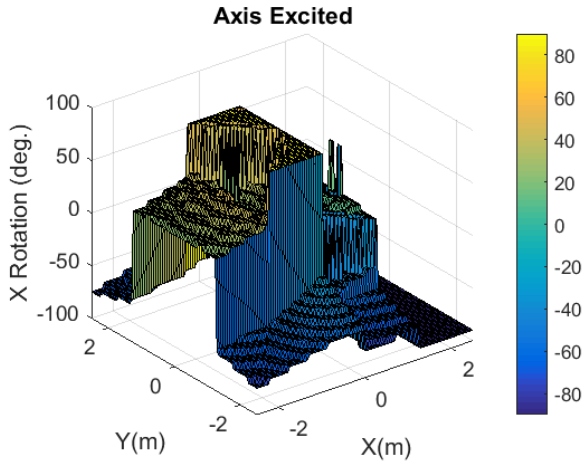

Fig. 9- The rotation angle limit in the x-z plane for the axis excited Tx pattern

the rotation angles around the y-axis, which results in the minimum P_r, has a pattern similar to Fig. 7 with a 90° rotation in the x-y plane, which is not shown here.

In the axis excited Tx model, the Txs have a rotated pattern compared to the corner excited topology and are located at (±1.25, 0, 3) and (0, ±1.25, 3) m. The minimum P_r in this topology is shown in Fig. 8. Compared to Fig. 6, it is observed that the minimum P_r show no significant changes at the center, but is increased in positions closer to the center. For example, the minimum P_r for the corner excited topology for the Rx's position of (0.5, 0, 0.85) m is -26.48 dBm, while in the axis excited pattern it is -24.44 dBm. Compared to SISO in Fig. 4, it is observed that the minimum P_r is increased in the corners. Fig. 9 shows the rotation angles around the x-axis, which leads to the minimum detectable power. It is observed that, the rotation angles were changed from -90° to 90°. The minimum P_r in the

location of (0, 0, 0.85) m is achieved by a rotation angle equal to 90°. The reason is that, for a 90° rotation around *x*, the Rx plane only receives data from the Tx located at (0, 1.25, 3) while it does not have access to the three other Rxs.

IV. CONCLUSION

In this paper, the Rx orientation was investigated for the VLC system for three different scenarios including SISO, MISO corner excited and MISO axis excited Tx's arrangements. For all scenarios, P_r was calculated by considering different rotation angles for a range of Rx's positions. The minimum P_r and also the rotation angles leading to the minimum P_r was then determined. In SISO, the results illustrated that, the minimum detectable P_r was increased up to -16 dBm at the center of the *x*-*y* plane, but was decreased at the corners and the rotation angle limits were between -90° and -25°. In the MISO corner excited, the detectable P_r was increased at the areas near to the corners, where the Txs were located, but compared to SISO the power was decreased at the center by 4 dBm. In this pattern, angle limits were changed between -90° and 90°. For MISO axis excited, compared to SISO, the results demonstrated that the minimum P_r was increased in the corners, and also compared to the corner excited model, it was increased in the areas near to the center. The angle limits were changed between -90° and 90°. As a conclusion, it is observed that the MISO models showed more flexibility when considering the Rx's orientation. Finally, we showed that between the two MISO models, the axis excited pattern offered an improved performance in terms of the minimum detectable P_r.

V. REFERENCES

[1] S. Dimitrov, H. Haas., "Principles of LED Light Communications: Towards Networked Li-Fi," Cambridge University Press, 2015.

[2] Uysal, M., Capsoni, C., Ghassemlooy, Z., Boucouvalas, A. and Udvary, E. eds., "Optical Wireless Communications: an Emerging Technology," Springer, 2016

[3] Z. Ghassemlooy, W. Popoola, S. Rajbhandari, "Optical Wireless Communications: System and Channel Modelling with MATLAB," Taylor & Francis, 2013.

[4] C. Le Bas, S. Sahuguede, A. Julien-Vergonjanne, A. Behlouli, P. Combeau, and L. Aveneau, "Impact of receiver orientation and position on visible light communication link performance," In Optical Wireless Communications (IWOW), (pp. 1-5), IEEE, 2015.

[5] J. Yan, and B. Zhu, "A visible light communication indoor localization algorithm in rotated environments," In computer, information and telecommunication systems (CITS), International Conference on, IEEE, 2016, pp. 1-4.

[6] W.A Cahyadi, Y.H. Kim, Y.H. Chung, and C.J. Ahn, "Mobile phone camera-based indoor visible light communications with rotation compensation," IEEE photonics journal, vol. 8, no. 2, 2016, pp. 1-8.

[7] J. Jeong, C.G. Lee, I. Moon, M. Kang, S. Shin, and S. Kim, "Receiver angle control in an infrastructure-to-car visible light communication link," in Region 10 Conference (TENCON), 2016 IEEE, pp. 1957-1960.

[8] J. Yan, Y. He, B. Zhu , and L. Chen, "Mobile device orientation estimation using visible light communication system," in Navigation Conference (ENC), 2016 European , 2016, IEEE, pp. 1-5.

[9] M. D. Soltani, X. Wu, M. Safari, and H. Haas, "Access point selection in Li-Fi cellular networks with arbitrary receiver orientation," In Personal, Indoor, and Mobile Radio Communications (PIMRC), 2016 IEEE 27th Annual International Symposium on, pp. 1-6.

[10] R. Zhang, W. D. Zhong, Q. Kemao, and Sheng Zhang, "A single LED positioning system based on circle projection.", IEEE Photonics Journal, vol 9, no. 4, 2017, pp. 1-9.

[11] M.D. Soltani, H. Kazemi, M. Safari, and H. Haas, "Handover modeling for indoor Li-Fi cellular networks: the effects of receiver mobility and rotation," In Wireless Communications and Networking Conference (WCNC), IEEE, 2017, pp. 1-6.

[12] S. Muhammad, "Delay profiles for indoor diffused visible light communication," 13th International Conference on Telecommunications (ConTEL), 2015, pp. 1-5.

[13] T. Ganjian, G. Baghersalimi, and Z. Ghassemlooy, "Performance evaluation of the received power based on the transmitter position in a visible light communications system," Iranian Conference on Electrical Engineering (ICEE), 2017, pp. 1763-1768.